IRIS AperTO

UNIVERSITÀ DEGLI STUDI DI TORINO

AperTO - Archivio Istituzionale Open Access dell'Università di Torino

Cooperative effects at water-crystalline silica interfaces strengthen surface silanol hydrogen bonding. An ab initio molecular dynamics study

This is the author's manuscript

Original Citation:

Availability:

This version is available http://hdl.handle.net/2318/125932 since 2016-08-07T18:12:32Z

Published version:

DOI:10.1039/c2cp40756f

Terms of use:

Open Access

Anyone can freely access the full text of works made available as "Open Access". Works made available under a Creative Commons license can be used according to the terms and conditions of said license. Use of all other works requires consent of the right holder (author or publisher) if not exempted from copyright protection by the applicable law.

(Article begins on next page)

12 October 2024

This is the author's final version of the contribution published as:

F. Musso; P. Mignon; P. Ugliengo; M. Sodupe. Cooperative effects at water-crystalline silica interfaces strengthen surface silanol hydrogen bonding. An ab initio molecular dynamics study. PHYSICAL CHEMISTRY CHEMICAL PHYSICS. 14 (30) pp: 10507-10514.
DOI: 10.1039/c2cp40756f

The publisher's version is available at:
http://xlink.rsc.org/?DOI=c2cp40756f

When citing, please refer to the published version.

Link to this full text:
http://hdl.handle.net/2318/125932

This full text was downloaded from iris - AperTO: https://iris.unito.it/

iris - AperTO

University of Turin's Institutional Research Information System and Open Access Institutional Repository

Cooperative effects at Water - Crystalline Silica Interfaces Strengthen Surface Silanol Hydrogen Bonding. An ab initio Molecular Dynamics Study

Federico Musso,[a,b] Pierre Mignon,[c] Piero Ugliengo[b*] and Mariona Sodupe[a*]

[a]*Departament de Quimica, Universitat Autònoma de Barcelona, Bellaterra 08193, Spain,*

[b]*Dipartimento di Chimica and NIS – Nanostructured Interfaces and Surfaces – Centre of Excellence, Università degli Studi di Torino. Via P. Giuria 7, 10125 Torino, Italy*

[c]*Université de Lyon; Université Claude Bernard Lyon1; Institut des Sciences Analytiques, CNRS UMR 5280; 43 Bd du 11 novembre 1918; 69622 Villeurbanne, Cedex, FRANCE*

[*]Corresponding author. E-mail:mariona.sodupe@uab.cat; piero.ugliengo@unito.it

Abstract

Silica and silica based materials are widely used in chemistry and material science due to their importance in many technological fields. The properties of these materials, which are crucial for their applications, are mainly determined by the presence of hydrogen bonding between surface silanols. Here, we present ab initio molecular dynamics simulations (AIMD) on different surfaces derived from the crystallographic α-quartz (100) and the α-cristobalite (001) and (101) faces, both free and at the interface with liquid water. The focus was on studying whether water adsorption can disrupt the H-bond pattern at the pristine free silica surface and how deep the perturbation due to the contact with the surface affects the structure of the water multilayer. Results highlight that the water phase is over structured at the interface with silica, as compared to water bulk. Furthermore, an apparent counterintuitive behavior has been observed for quartz (100) and cristobalite (001) surfaces: the interaction with water does not cleave the pre-existent H-bonds between the surface silanol groups. On the contrary, in several cases, it is observed that SiOH···OHSi H-bonds are even strengthened, as the result of a mutual cooperative H-donor/H-acceptor enhancement between silanols and water molecules, which may alter the adsorption capability of these silica surfaces.

1. Introduction

Silica and silica based materials are widely used in chemistry and material science due to their importance in many technological fields such as chromatography, microelectronic, metal-supported catalysis and medicine.[1, 2] In most cases, the essential role of these materials is more determined by the surface properties than by the bulk. For instance, molecular sieves such as MCM-41[3, 4] show high surface areas and high pore volumes, which make them very attractive supports for the adsorption or binding of biologically relevant molecules in confined spaces as controlled-drug-delivery systems.[5]

The interactions between silica surfaces and molecules present in the external environment are mainly driven by two functionalities of different nature: silanols (Si-OH), which interact with hydrophilic molecules through hydrogen bonding, and siloxane bridges (Si-O-Si), which interact with hydrophobic molecules through dispersive forces. Experimental techniques such as ^{29}Si NMR and IR spectroscopy are able to distinguish the different nature of surface functionalities such as isolated, geminals or hydrogen bonded siloxanes or silanols.[6] However, they do not provide structural details of the local topology of these groups at the surface of different silica polymorphs. Molecular modeling may compensate this lack of information and, actually in the last ten years the surface properties of silica materials have been increasingly studied theoretically.[5, 7-21] For instance, quantum mechanical studies on fully hydroxylated surfaces of both crystalline and amorphous high-density silica polymorphs [22, 23] highlight that their differences result from the different pattern of hydrogen bonding between the silanols present at the surface. In fact, due to the translational symmetry, crystalline surfaces with a high degree of hydroxylation often show expanded hydrogen bond chains. On the other hand amorphous silica with similar hydroxylation degree tends to present localized hydrogen bonds in confined areas.

These properties, however, have been described in vacuum at 0K, whereas technological relevant processes occur in a water-rich environment at room temperature. So, both the effect of temperature and the presence of water at the interface are of paramount importance since they can strongly modify the properties of pristine silica surfaces. The aim of the present work is to study the surface properties of silica at the interface with liquid water, treating the effect of the solvent in an explicit way, by means of DFT ab initio molecular dynamics (MD).

The silica-water interface, including a large number of water layers, has been described in some computational studies, most of them using classical MD [24-30] and few with ab initio MD.[31-35] Recently Skelton at al.[34, 35] studied the silica-water interface by ab initio MD, considering two surface terminations, *e.g.* with hydrogen bonded and non-hydrogen bonded silanols. This study shows that the two terminations exhibit a significant different behavior due to differences in connectivity and surface hydrogen bonding, which may influence the resistance to dissolution of the different surfaces. Here we consider three different surfaces derived from quartz and cristobalite silica polymorphs that contain exposed silanols of different nature, e.g. with silica units with Q^2 (two OH and two siloxanes) and Q^3 (one OH and three siloxanes) terminations, all of them involved in hydrogen bond interactions of different H-bond patterns (single H-bonds or H-bond chains). Three different aspects of interest will be considered here: i) the change in H-bonds when the surfaces are in contact with liquid water, ii) the extent to which the water multilayer is significantly perturbed from bulk water behavior due to the contact with the surfaces and iii) the dependency of the perturbation on the considered surface. The first of these three questions is of particular interest since it will largely influence the adsorption properties in solution.

2. Computational details

2.1 Level of theory

The present study is based on periodic models computed with the VASP code,[36, 37] which can perform MD simulations based on the Density Functional Theory. All the calculations have been performed considering the projector augmented wave method (PAW)[38, 39] to describe the ionic cores and plane waves to describe valence electrons. The adopted functional is the PBE exchange correlation functional,[40] with a kinetic energy cutoff for plane waves of 400 eV. The PBE hamiltonian and the plane wave cutoff of 400 eV have been chosen according to previous works on bulk water and periodic silica models studied within a plane wave approach.[19, 41-43] In particular, for crystalline silica, the study of Goumans et al.[19] on the (001) surface of quartz shows that PBE and B3LYP structures, calculated with plane waves and Gaussian orbitals, respectively, are in close agreement with each other and also in good agreement with the B3LYP structure of the same system, proposed by us.[23] In fact, for quartz (001), our B3LYP study and that of Goumans at the PBE level of theory, using plane waves, show the very same H-bond pattern at the surface and a maximum variation of 10% in length for the weaker H-bond. Molecular dynamics calculations have been carried out sampling the Brillouin zone at Γ-point only, due to the large cells involved (see Figure 1).

2.2 Models

The surface models, studied with a periodic approach, have been built by cutting out a slab of a given thickness from the bulk structures of α-quartz and α-cristobalite. The unsatisfied Si and SiO valences resulting from the cut were filled with OH groups and H atoms, respectively, with the MOLDRAW graphic program,[44] in order to obtain fully hydroxylated surface models. The three crystalline surfaces considered are the (100) surface of α-quartz, hereafter referred to Q(100), and the (001) and (101) models

of α-cristobalite labeled as C(001) and C(101). Note that the hydroxyl density of C(101) is ρ~5 OH/nm^2, whereas that of the Q(100) and C(001) surfaces is ρ~7.7 and 8.5, respectively.

The cell parameters for every slab have been defined in this way: bulk structures of quartz[45] (ICSD 93974) and cristobalite[46] (ICSD 77452) have been fully optimized (cell and atomic coordinates) with a cutoff of 1000 eV, which ensures the convergence of the bulk structure when the cell volume and shapes change. Then the surfaces where defined in such a way that the cell vectors, *a* and *b*, are twice the size of the primitive bulk cell vectors (see Figure 1). Finally, the atomic coordinates of each surface model have been optimized keeping the defined cell fixed at the values from the bulk optimization (*vide supra*). The three structures present the same hydrogen bond patterns, with very similar geometrical properties than those previously calculated at the B3LYP/G-31G(d,p) level of theory.[23]

With VASP the slab is artificially replicated along the direction perpendicular to the *(hkl)* plane, so that the cell vector *c* must be defined. In the three cases the *c* value was set to 35 Å, which minimizes the spurious interactions between the slab replicas. The thickness of the slabs, 12.5 Å, is the same for the three cases. The three optimized structures are represented in Figure 1 (only the top face is shown since the bottom face is identical). Note that Q(100) and C(101) models present silanols arranged in infinite H-bond chains, whereas C(001) presents geminal silanols with four single strong H-bonds per cell.

In order to study the silica-water interface with ab initio MD, a water box of ~20 Å of thickness has been positioned at 2.5 Å from each surface in such a way that water molecules fill the empty space between the two slabs along the *c* direction. This way, the water phase remains confined between two silica surfaces, as represented in Figure 2. The water box has been built starting from the Ih structure of ice (Space group

Pna21). A box of 1 nm^3 containing 32 ice-ordered water molecules has been disordered performing 1000 fs of molecular dynamics at 300K. The obtained structure has been used to build the box of dimension $a*b*20$ $Å^3$ (Figure 2), where *a* and *b* are the cell parameters of the considered silica surfaces. The thickness of the water layer (~20 Å) has been chosen in order to describe approximately six shells of water molecules, so that, for each one of the confining silica surfaces, there is a first shell of water in direct contact with the silica phase, then a second and third shell which are in contact with other water molecules. The number of water molecules inside the box of volume ($a*b*20$) $Å^3$ is 63, 52, and 68 for C(001), C(101) and Q(100) respectively, which corresponds to a water density of equal to ~1.00, 0.97, and 0.98 g/ml.

2.3 MD simulations

In order to find a reasonable starting point for the subsequent ab initio MD simulations, water molecules inside the cell were first relaxed while keeping fixed the coordinates of silica atoms. This way the dynamics equilibration starts with the water phase in its minimum configuration, while maintaining the surface H-bonds obtained from the previous optimization in vacuum. Then, MD simulations of the Q(100), C(001) and C(101) hydrated surfaces were carried out considering an equilibration period of 1 ps (1000 steps of 1 fs), at fixed temperature (T=300K), within the canonical ensemble (NVT). During this period atomic velocities are scaled to the temperature and the initial velocities are selected according to the Boltzmann distribution. Then, a production time of 10 ps (10000 steps of 1 fs) was carried out within the microcanonical ensemble (NVE). The production time of 10 ps, even if slightly short, allows us to analyze if H-bonds on the surface are broken or if, in contrast, weak contacts occur between the solid and the liquid phase, thereby indicating that, despite being hydroxylated, the silica surface shows a substantial hydrophobic behavior.

During both the equilibration and production periods the inner atomic layers of the silica slabs were maintained at fixed positions, while only the external O_3SiOH tetrahedra and water molecules were allowed to move according to the motion's equations. We chose this option to avoid unrealistic deformation of the internal structure of the slabs, since real silica surfaces are linked to a macroscopic bulk.

3. Results

The results are divided into two different parts. We will first focus on the water structure (both bulk and interface structures). Second, we will address the silica-water interface and the influence of temperature and water on the surface properties, especially on the changes induced on the hydrogen bonding between silanols.

3.1 The water structure

In order to analyze the properties of liquid water at the interface different kinds of atomic species have been defined: O_w and H_w represent water oxygen and hydrogen atoms and O_s and H_s the oxygen and hydrogen atoms of the exposed ≡ SiOH silanols. The water structure is analyzed considering radial distribution functions (RDF) and the density profile of water molecules along vector *c*, perpendicular to the surface.

In Table 1 the position of the first peak of O_w-O_w, O_w-H_s, O_s-H_w RDFs and the first peak of non-bonded O_w-H_w RDF are reported. These values describe the distance between oxygen atoms of adjacent water molecules (O_w-O_w), and the distances of the water-silanol (O_s-H_w), silanol-water (O_w-H_s), and water-water (O_w-H_w) hydrogen bonds. The position of the O_w-O_w peak reported in Table 1 is in very good agreement with X-ray studies of the structure of liquid water[47, 48] (2.73 Å) and with previous DFT analysis of liquid water performed with the same functional, in similar computational conditions[41-43, 49] (2.70-2.75 Å). These values are also in very good agreement with those calculated by some of us in the study of hydrated cations in montmorillonite[50]

(2.72-2.74 Å). The coordination number of the oxygen atom of water molecules is calculated by counting the number of coordinated water molecules per O_w atom up to the first minimum of the RDF. The values, listed in Table 1, are 3.7 for Q(100) and C(001) and 3.8 for C(101), somewhat smaller than that previously calculated (4.3) in bulk water.[41]

Figure 3 shows the calculated O_w-O_w RDFs as well as the density of water molecules along the *c* vector, for the water-silica systems. Moreover, and for the sake of comparison, we have also included the values corresponding to a box of pure water; i.e. a box that contains 32 water molecules and exhibits a density equal to 0.96 g/ml. As previously observed by Mignon et al.,[50] the calculated O_w-O_w RDFs of the three systems present a more defined second peak with a maximum at around 4.5 Å (see Figure 3 left), as compared to the RDF obtained from X-ray scattering experiments.[48] The presence of this pronounced peak is due to the fact that the water phase is over-structured, as also confirmed by the density of water molecules along the *c* vector, perpendicular to the surface (see Figure 3 right). In fact, the plot of the O_w density along the *c* axis, over the 10000 steps (solid lines in Figure 3 right) shows several pronounced peaks separated by a distance of ~3Å, which is approximately the distance between H-bonded water molecules. Although this over structured water is partly due to the enhancement of H-bond strength between water molecules at the PBE level,[41-43] the comparison between silica-water systems (Figures 3b-3d) and pure water (Figure 3a) indicates that water appears to be more structured in contact with silica. This is in agreement with previous works,[27, 28] which have remarked that an ordered (ice-like) structure of water appears at the interface with silica, up to a distance of approximately 12-14 Å from the surface.

The comparison between the different surfaces indicate that over structuration of water is more pronounced for Q(100) and C(001), for which the two external peaks of

the water density are sharpen and higher than the central ones (Figure 3). This suggests that water molecules in contact with silica show less mobility, the silica-water H-bonds being stronger than those between water molecules in the central part of the water phase. The C(101) model shows a different behavior since the external water layers in contact with silica do not appear to be more structured as compared to the central ones, the peaks of O_w being of the same height. This may be the result from the lower silanol density on C(101) (ρ~5 OH/nm^2) with respect to Q(100) and C(001) surfaces (ρ~7.7 and 8.5, respectively, see Figure 1), which leads to less silanol-water interactions in the water silica interface.

The presence of a O_s-H_w peak at 1.74, 1.78 and 1.82 Å and a O_w-H_s peak at 1.65, 1.63 and 1.66 Å for Q(100), C(001) and C(101) (see Table 1), respectively, shows the formation of hydrogen bonds between water molecules and silanols at the interface, with water molecules acting both as donor and acceptor. It is worth noting that the O_w-H_s distances are shorter than the O_s-H_w and O_w-H_w ones, in agreement with the higher acidity of silanols. Note that the pK_a values of silanol groups have been measured to belong to two different groups with values of ~4.5 and ~8.5, respectively.[51-53] On the other hand, the existence of the O_w-H_s peak suggests that the intramolecular H-bonds between silanols on the free surfaces have probably been disrupted at the silica-water interface. Indeed, the external O_w peaks on both sides and the peak that describes the position of exposed-silanol oxygen atoms (O_s, dotted line) are 3 Å apart, i.e., at a proper distance to establish H-bond contacts.

3.2 The silica structure

To start with, we performed short molecular dynamics (1000 steps of 1 fs of production) at T=300K on dry Q(100) and C(101) surfaces in order to assess whether

the H-bond pattern of each model at room T coincides with the one resulting from geometry optimization at 0 K. Starting geometries correspond to the optimized structures at 0K. Table 2 reports the H-bond values obtained from geometry optimization for the three silica slabs, $(H_s\cdots O_s)^{opt}$, the average value of the same H-bond along the 1000 steps of the dynamics at the dry Q(100) and C(101) surfaces, $<H_s\cdots O_s>^d$, and the average H⋯O distances when the surfaces are in contact with the water phase, $<H_s\cdots O_s>^w$.

Q(100) in vacuum shows eight hydrogen bonds per surface (top and bottom) arranged in two infinite chains (see Figure 1). The two chains exhibit alternating groups of two strong (around 1.7 Å of length) and two weak (around 2.2 Å of length) hydrogen bonds. The $<H_s\cdots O_s>^d$ values show that the hydrogen bond pattern is mainly maintained even at 300K, the average H-bonds along the 1000 steps of the dynamics being very close to the values obtained from geometry optimization at 0K. Only the $<H_s\cdots O_s>^d$ distances marked in Figure 1 as 4 and 8 are definitely elongated with respect to the $(H_s\cdots O_s)^{opt}$ values at 0K, passing from 2.20 Å to 2.41 Å and from 2.20 Å to 2.49 Å, respectively. Such differences are due to the fact that these two weak H-bonds show larger fluctuations during the dynamics as effect of the temperature. In the case of C(101) slab, the $<H_s\cdots O_s>^d$ values, both on the top and the bottom surfaces, are considerably larger than the $(H_s\cdots O_s)^{opt}$ ones, indicating that a temperature of 300K provokes the disruption of all the hydrogen bonds along most part of the dynamics simulation. In general, results in the first and second column of Table 2 highlight that the stronger hydrogen bonds (<2 Å) obtained at 0K are all maintained at 300K whereas weaker hydrogen bonds (>2 Å) are maintained in some cases and lost in other. A similar behavior is expected for dry C(001) slab; i.e., the strong H-bonds will probably be retained at 300K.

Let's now consider how surface H-bonds change when silica is in contact with water. The $<H_s\cdots O_s>^w$ values of Table 2 show that for every different chain the stronger H-bonds are maintained in the presence of water, whereas the weaker ones are broken, favoring the interaction of donor silanols with water molecules. Figure 4a shows the evolution of the H-bonds forming the chain 1-4 (see Figure 1) when the surface is in contact with water. For the sake of clarity only chain 1-4 is showed, the behavior of the rest of the hydrogen bonds, both on the top and the bottom surfaces, being equivalent to those showed.

In the case of C(001) slab, results indicate that the four strong H-bonds are maintained even in the presence of water, the $<H_s\cdots O_s>^w$ values being very close to the optimized $(H\cdots O)^{opt}$ ones. Note that H-bonds labeled as 1 and 3 (see Figure 1) of the bottom surface are broken during some steps of the simulation, the donor silanols being involved in hydrogen bonding with the surrounding water molecules. The evolution of these two H-bonds is represented in Figure 4b which shows that, despite occasional breaks, the two H-bonds on silica remain under a value of 2 Å during the largest part of the simulation, their average values being 1.73 and 1.76, (see Table 2).

From Table 2 it can also be observed that the elongated hydrogen bonds at the C(101) surface, arranged in an infinite chain in vacuum are lost in the presence of water, the $<H_s\cdots O_s>$ values being larger than 3.5 Å. In spite of that, the evolution of the H···O distances highlights that some H-bonds at the silica surface are conserved during the dynamics simulation (see Figure 4c). In fact, silanols which are involved in H-bonds 1 and 3 at the bottom surface (see Figure 1), are kept even in contact with water, but now with a reversed role of the two silanols: the one which was originally acting as donor becomes the acceptor whereas the original acceptor one becomes the donor. The two new contacts show average values of ~2.14 and ~2.30 Å during 8000 of the total 10000 steps of dynamics production (see Figure 4c).

Another interesting aspect is evidenced in Table 2. In the case of Q(100) and C(001) some $<H_s\cdots O_s>^w$ values are shorter than the optimized H⋯O distances; i.e., in some particular cases surface H-bonds appear to be strengthened upon entering in contact with water. The effect is even larger for Q(100) where, for instance, H-bond 1 is strengthened both on the top and the bottom surface, passing from 1.73 (1.72) Å to 1.68 (1.66) Å, H-bond 3 on the top surface vary from 1.73 Å to 1.66 Å, and H-bond 7 on the top surface from 1.73 Å to 1.64 Å. In all this cases, the ≡ SiOH ⋯ OHSi ≡ bonds are involved in a cooperative interaction with several water molecules in such a way that silanols and water molecules are involved in donor and acceptor interactions defining hydrogen bond rings as the one described in Figure 5a. Thus, silanol groups are linked together at the silica surface.

In order to further investigate this aspect we run a dynamics simulation for Q(100) slab interacting with water, but removing any constraint to the internal atomics layers of the silica slab. The hydrogen bond cooperative effect between silanols and water is even enhanced, the H-bond chains showed by Q(100) in vacuum being somehow maintained. For instance the chain formed by H-bonds 1-2-3 of Figure 1 is preserved with average <H⋯O> distances of ~1.7, ~1.9 and ~1.7, respectively. The situation is represented in Figure 5b. Thus, these results suggest that exposure to water does not weaken the intramolecular hydrogen bonding between surface silanols, but, in fact, strengthen them due to cooperative effects with the surrounding water molecules. This is a very interesting aspect that extends some ideas that emerged in a previous work,[54] where we discussed how the adsorption energy of a single water and ammonia molecule depends on the presence and strength of H-bonds between silanols of the naked surface, since surface H-bonds must be broken in order to establish new H-bonds with the adsorbed molecule.

The H-donor/H-acceptor behavior of hydroxyls involved in hydrogen bond chains or rings, as those described in Figure 5, result from changes on electron density upon interacting with nearby molecules. That is, the oxygen basicity of a hydroxyl group acting as hydrogen bond donor is increased with respect to that of an oxygen atom belonging to a non-interacting OH group, which provokes a strengthening of the H-bond in which the same oxygen is involved as acceptor. The same effect is expandable to all the elements of the ring which cooperate one with each other.

The role of H-bond cooperativity may be assessed by calculating the H-bond distance of a pair of silanols in mutual H-bond interaction, the net charge on the hydrogen atoms behaving as H-donor and the frequency shift undergone by the OH stretching donor in the presence of a different number of water molecules arranged to give H-bond rings of increasing size. Considering cluster calculation in gas phase, the starting structure a) of the two interacting silanols has been freely optimized, whereas for structures b)-d) the two SiH_3 moieties have been kept fixed at the optimized positions of structure a) in order to mimic the constraints imposed by the surface. The shortening of the intermolecular O···H distance between the two silanols, the increase of the frequency shift of the OH stretching donor and the increase of the Mulliken charge on the H donors are signs of H-bond cooperativity as shown in previous works.[55-63] Indeed, the O···H bond distance calculated at the PBE level with a triple ζ polarized basis set of Ahlrichs and coworkers,[64] decreases from 1.85 Å for structure b) to 1.75 for c) and 1.71-1.72 for structures d)-f). In addition, the values of the Mulliken net charges for the silanol H donor also increase regularly (from 0.31 for b) to 0.34-0.35 for c)-f)), as well as the frequency shift undergone by the OH stretching donor, as expected when H-bond cooperativity is present. As found previously, major cooperative effects appear for the cyclic structures,[55] for which the vibrational shift of the OH donor is more than double than that observed for the dimer.[58] It is worth noting that this subtle

charge-transfer and polarization effect (which is expected also to occur for the plane waves ab initio MD calculations) cannot be described with classical force fields unless they are polarizable and explicitly account for many body induction effects.[65, 66]

4. Conclusions

In the present paper we describe the properties of some crystalline silica surfaces (Q(100), C(001) and C(101)) at the interface with water, by means of ab initio molecular dynamics simulations. The models considered include six layers of water molecules confined between two silica surfaces which are almost identical. The analysis of the density of water molecules at the interface reveals that the presence of the silica induces an ice-like structure of water in the proximity of the surface. This ice-like structure appears to be more pronounced when the silanol density at the surface is higher, as shown for Q(100) and C(001). Moreover, results show that weak hydrogen bonds between surface silanols (H···O > 2Å) can be easily broken by the effect of the temperature and the surrounding water molecules. On the contrary, the stronger H-bonds (H···O < 2Å) are always preserved. Furthermore, the strength of these hydrogen bonds can be, in some cases, enhanced due to cooperative H-bond effects established between silanols and the surrounding water molecules, which leads to the formation of hydrogen bond rings.

The strengthening of silanol H-bonding upon interacting with water is a very interesting aspect with important consequences, since the breakage of silanol-silanol hydrogen bonds may result even more difficult in the presence of water at the interface, reducing the adsorption capability of the silica material. This behavior appears to be more relevant for those surfaces with a high degree of hydroxylation because silanols are closer allowing for stronger H-bonds. Overall, present study shows that the surface properties of silica materials cannot be exclusively understood from magnitudes such as

the OH density. H-bond properties, which differ according to the polymorph or the crystalline plane, can play a major role.

Acknowledgements

Financial support from MICINN (CTQ2011-24847) and BSC-MN for generous allowance of computing time (QCM-2008-1-0012) are gratefully acknowledged. F. M. thanks the Ministerio de Ciencia e Innovación for a FPU fellowship.

Table 1: Position of the first peak (Å) of the RDF of silica-water interface models and coordination number of water oxygen. For O_w-H_w, the intramolecular bonds are not considered.

	Q(100)-H_2O	C(001)-H_2O	C(101)-H_2O
O_w-O_w	2.71	2.72	2.71
O_w-H_w	1.76	1.76	1.74
O_s-H_w	1.74	1.78	1.82
O_w-H_s	1.65	1.63	1.66
O_w Coord. nb.	3.7	3.7	3.8

Table 2. Comparison between the $(H_s\cdots O_s)^{opt}$ distances, average $<H_s\cdots O_s>^d$ distances along 1000 fs point of dynamics for dry surfaces, and $<H_s\cdots O_s>^w$ distances along 10000 fs of the dynamics for water-crystalline silica interfaces. The H-bonds are labeled according to Figure 1, values in parenthesis represent the equivalent H-bond on the bottom surface.

		$(H_s\cdots O_s)^{opt}$	$<H_s\cdots O_s>^d$	$<H_s\cdots O_s>^w$
Q(100)	1	1.73 (1.72)	1.75 (1.75)	1.68 (1.66)
	2	2.22 (2.20)	2.28 (2.17)	3.47 (3.05)
	3	1.73 (1.71)	1.77 (1.72)	1.66 (1.72)
	4	2.20 (2.20)	2.28 (2.41)	4.12 (2.98)
	5	1.73 (1.72)	1.74 (1.73)	1.74 (1.75)
	6	2.22 (2.20)	2.23 (2.21)	3.56 (3.79)
	7	1.73 (1.71)	1.74 (1.77)	1.64 (1.71)
	8	2.19 (2.20)	2.29 (2.49)	3.89 (3.31)
C(001)	1	1.63 (1.64)	-	1.65 (1.73)[a]
	2	1.63 (1.64)	-	1.66 (1.63)
	3	1.63 (1.64)	-	1.62 (1.76)[a]
	4	1.64 (1.64)	-	1.63 (1.73)[a]
C(101)	1	2.20 (2.23)	2.30 (2.93)	3.66 (3.51)
	2	2.14 (2.14)	2.93 (2.45)	2.28 (3.54)
	3	2.24 (2.25)	2.56 (2.90)	3.80 (3.68)
	4	2.17 (2.15)	2.56 (2.82)	3.78 (3.50)

[a] Values larger than 2.0 Å for more than 10 fs have been excluded when calculating the average. See Figure 4b.

Figure captions

Figure 1: Q(100), C(001) and C(101) surface models which atomic coordinates have been optimized at fixed cell. Cell vectors got from quartz and cristobalite bulk full-optimization. H-bonds are numbered for following analysis.

Figure 2: C(101)-water model used to study the silica-water interface. A layer of 20 Å is confined between the upper and lower surface of the C(101) slab model, replicated along the direction of vector *c*.

Figure 3: on the left radial distribution functions of water oxygen atoms (O_w-O_w); on the right water oxygen density along the *c* axis (the black dotted lines indicate the position of the external oxigen atoms of the silica surfaces, O_s).

Figure 4: H⋯O distance along the dynamics simulations with water (a) H-bonds 1-4 of Q(100) (continuous line: H-bonds 1 and 4; dotted line: H-bonds 3 and 2) (b) H-bonds 1 (continuous line) and 3 (dotted line) of C(001) (c) H-bonds of C(101) model: reversed hydrogen bonds with respect to the optimized structure are formed when the surface is in contact with water.

Figure 5: H-bond cooperation between silica and water molecule on Q(100) when the inner atomic layers of silica slab are maintained at fixed position (a) and when no constraint is applied to silica atoms (b).

Figure 6: OH and hydrogen bond distances (H⋯O) (in bold) for a) $H_3SiOH{\cdot\cdot}H_2O$ and different $(H_3SiOH)_2(H_2O)_n$ (n=0-4) clusters models at the B3LYP level of theory. For clusters c), d), e) and f) including one, two, three and four water molecules, respectively, the position of Si atoms and the Si-H bonds were fixed at the values obtained in b). Frequency shifts of the OH stretching donor are included in parenthesis.

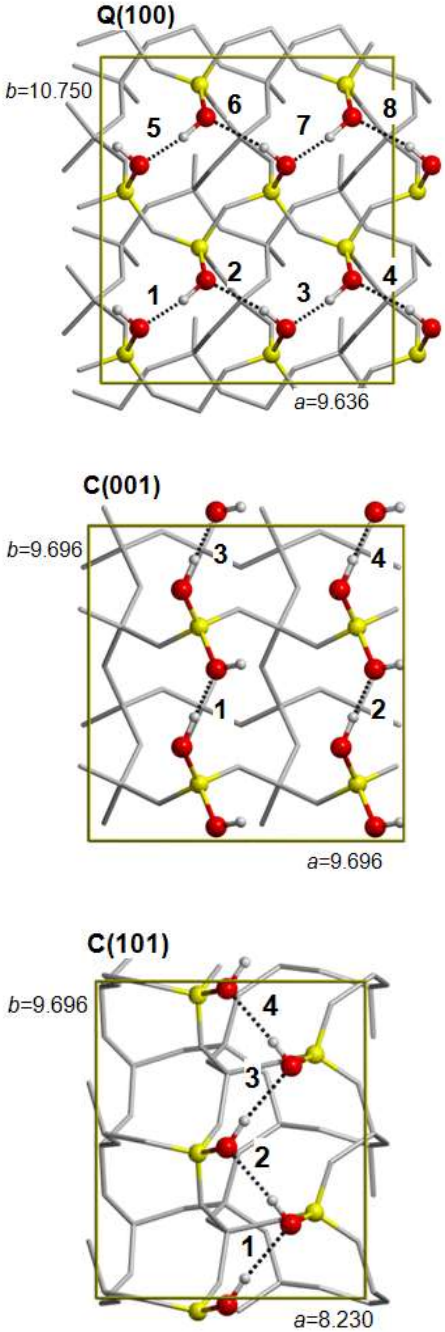
Q(100)
b=10.750
a=9.636
1
2
3
4
5
6
7
8
C(001)
b=9.696
a=9.696
1
2
3
4
C(101)
b=9.696
a=8.230
1
2
3
4

Figure 1

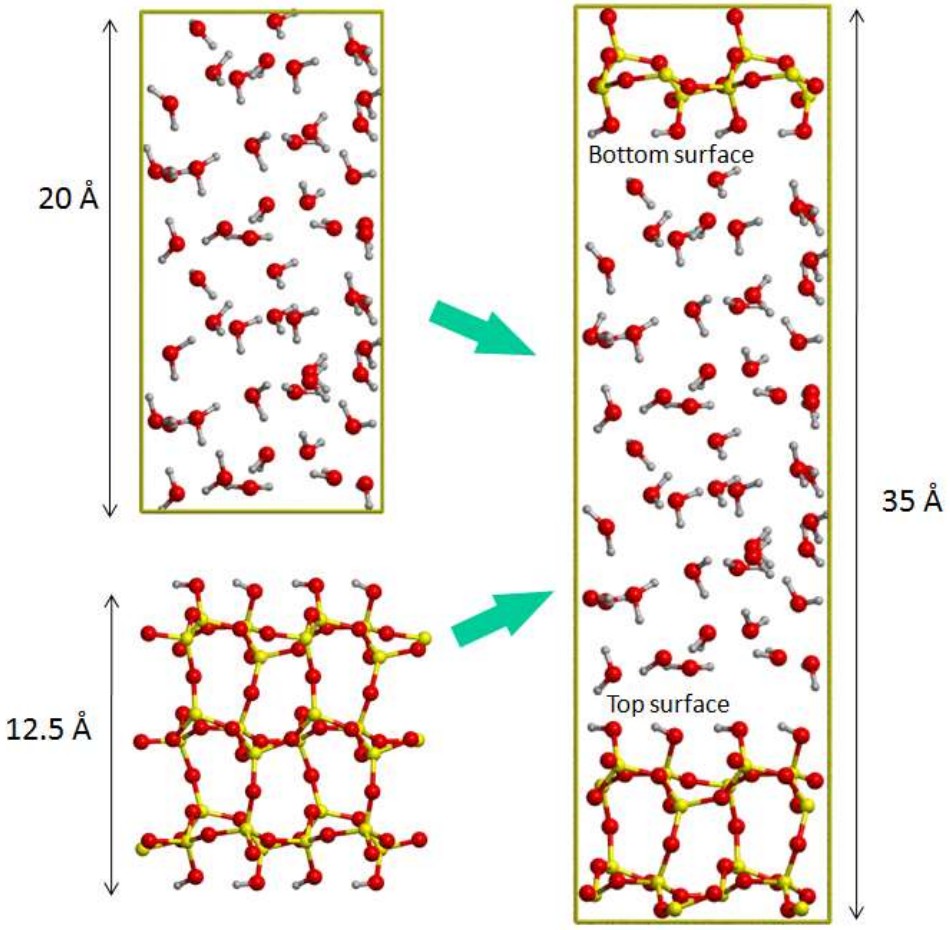

Figure 2

H_2O

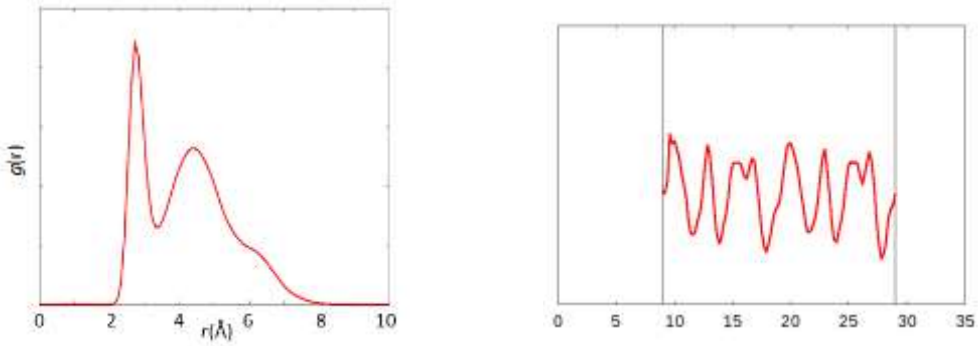

H_2O-Q(100)

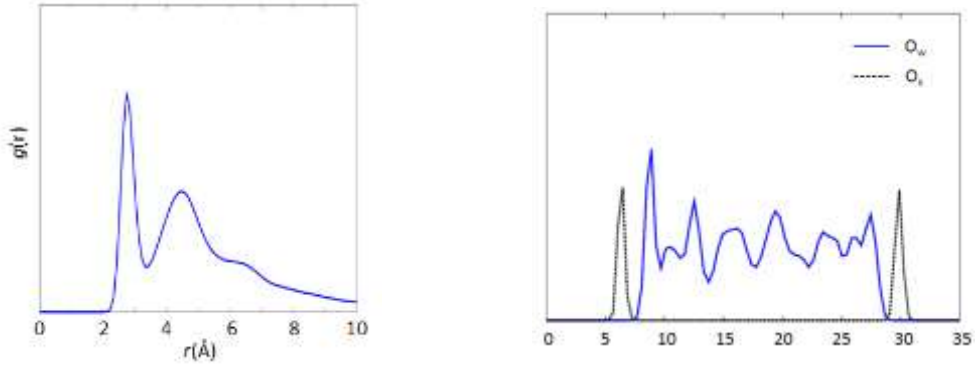

H_2O-C(001)

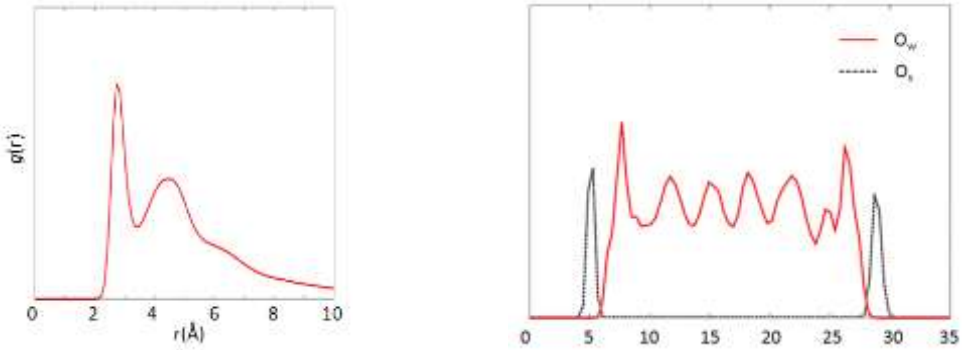

H_2O-C(101)

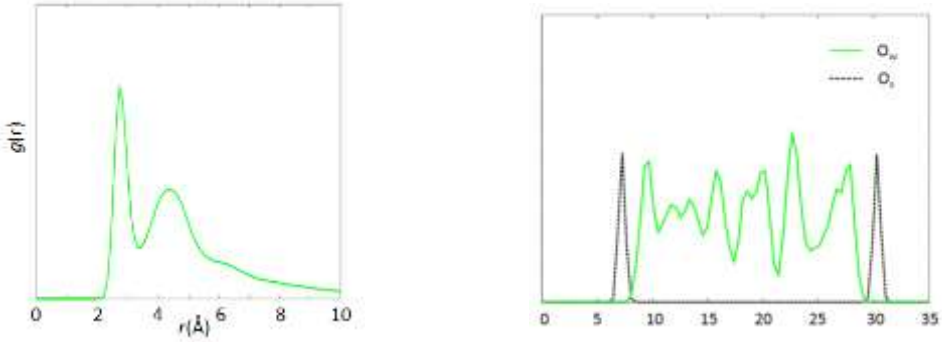

Figure 3

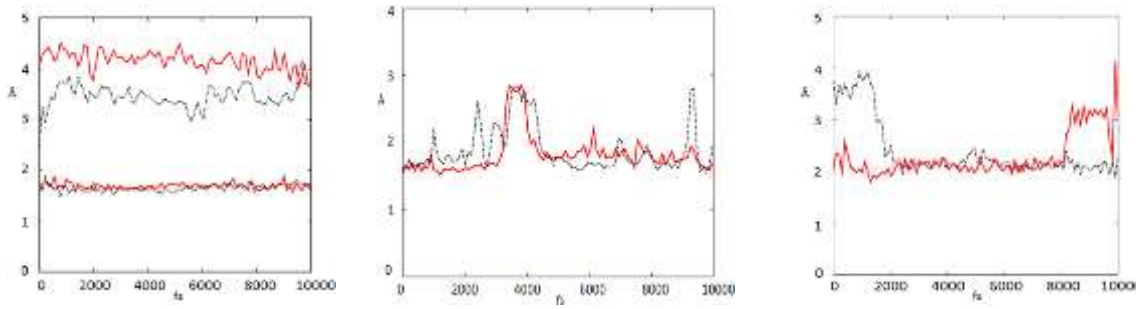

(a) (b) (c)

Figure 4

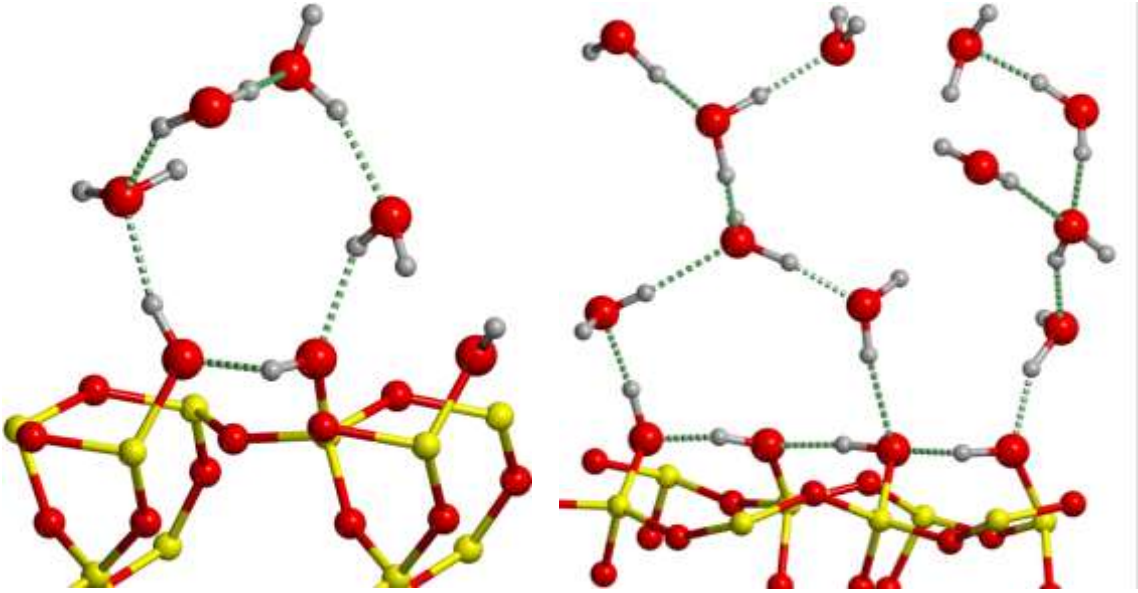

(a) (b)

Figure 5

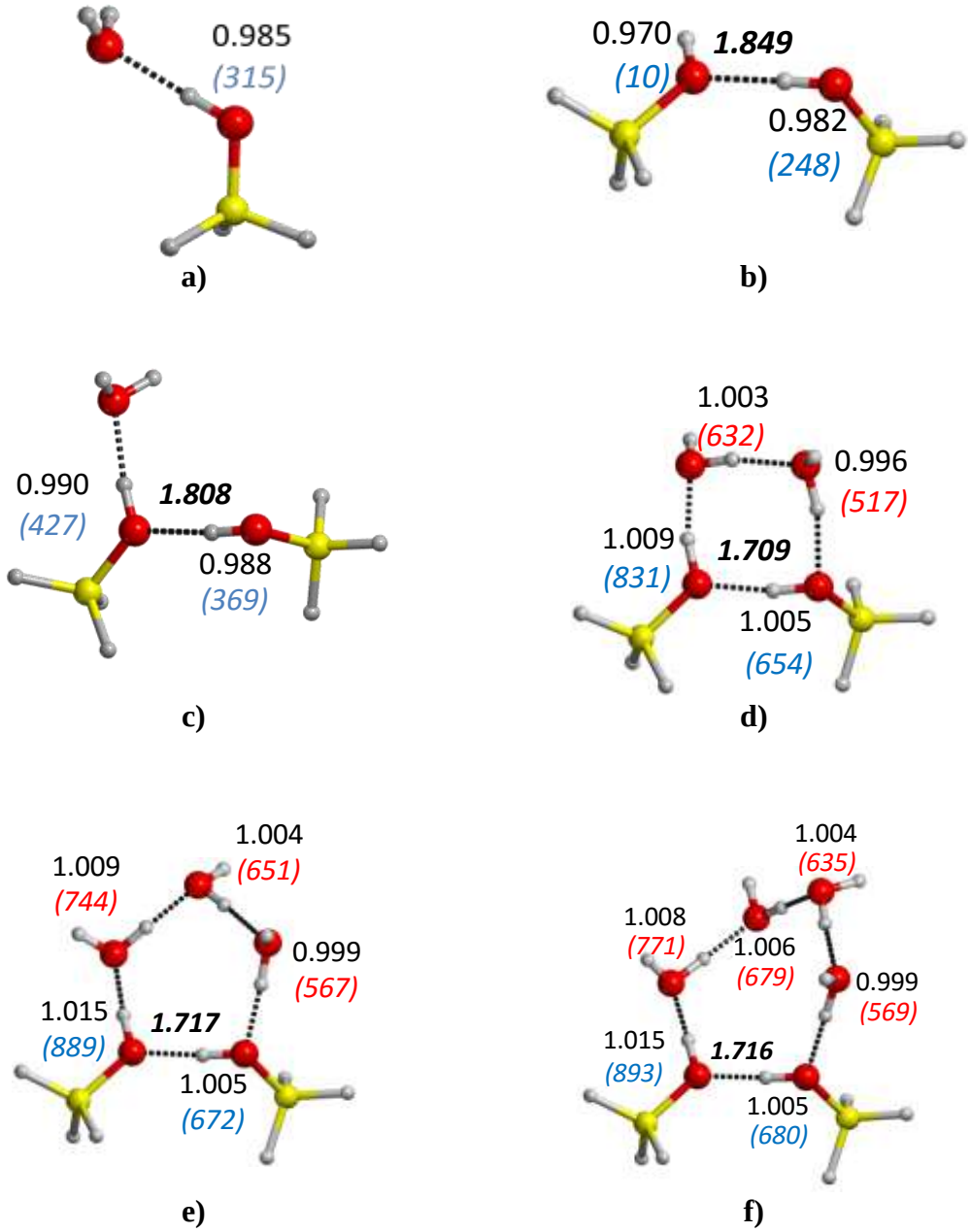
0.985
(315)
a)
0.970
(10)
1.849
0.982
(248)
b)
0.990
(427)
1.808
0.988
(369)
c)
1.003
(632)
0.996
(517)
1.009
(831)
1.709
1.005
(654)
d)
1.004
(651)
1.009
(744)
0.999
(567)
1.015
(889)
1.717
1.005
(672)
e)
1.004
(635)
1.008
(771)
1.006
(679)
0.999
(569)
1.015
(893)
1.716
1.005
(680)
f)

Figure 6

References

1. R. K. Iler, *The Chemistry of Silica: Solubility, Polymerization, Colloid and Surface Properties and Biochemistry*, Wiley-Interscience, New York, 1979.
2. M. Pagliaro, *Silica-Based Materials for Advanced Chemical Applications*, RSC Publishing, Cambridge, 2009.
3. C. T. Kresge, M. E. Leonowicz, W. J. Roth, J. C. Vartuli and J. S. Beck, *Nature*, 1992, **359**, 710.
4. J. C. Vartuli, K. D. Schmitt, C. T. Kresge, W. J. Roth, M. E. Leonowicz, S. B. McCullen, S. D. Hellring, J. S. Beck, J. L. Schlenker, D. H. Olson and E. W. Sheppard, *Chem. Mater.*, 1994, **6**, 2317-2326.
5. M. Vallet-Regí, F. Balas and D. Arcos, *Angew. Chem. Int. Ed.*, 2007, **46**, 7548.
6. B. A. Morrow and I. D. Gay, in *Adsorption on Silica Surfaces*, ed. E. Papirer, Marcel Dekker, New York, 2000, vol. 60, pp. 9-34.
7. F. Vigné-Maeder and P. Sautet, *J. Phys. Chem. B*, 1997, **101**, 8197-8203.
8. B. Civalleri, S. Casassa, E. Garrone, C. Pisani and P. Ugliengo, *J. Phys. Chem. B*, 1999, **103**, 2165-2171.
9. N. H. de Leeuw, F. M. Higgins and S. C. Parker, *J. Phys. Chem. B*, 1999, **103**, 1270-1277.
10. D. Ceresoli, M. Bernasconi, S. Iarlori, M. Parrinello and E. Tosatti, *Phys. Rev. Lett.*, 2000, **84**, 3887.
11. B. Civalleri and P. Ugliengo, *J. Phys. Chem. B*, 2000, **104**, 9491-9499.
12. G. M. Rignanese, A. De Vita, J. C. Charlier, X. Gonze and R. Car, *Phys. Rev. B*, 2000, **61**, 13250-13255.
13. S. Iarlori, D. Ceresoli, M. Bernasconi, D. Donadio and M. Parrinello, *J. Phys. Chem. B*, 2001, **105**, 8007-8013.
14. G. M. Rignanese, J. C. Charlier and X. Gonze, *Phys. Chem. Chem. Phys.*, 2004, **6**, 1920-1925.
15. M. Casarin, D. Falcomer, A. Glisenti, M. M. Natile, F. Poli and A. Vittadini, *Chem. Phys. Lett.*, 2005, **405**, 459-464.
16. V. V. Murashov and E. Demchuk, *J. Phys. Chem. B*, *2005*, ***109***, 10835-10841.
17. J. J. Yang, S. Meng, L. F. Xu and E. G. Wang, *Phys. Rev. B*, 2005, **71**.
18. J. Yang and E. G. Wang, *Phys. Rev. B*, 2006, **73**, 035406.
19. T. P. M. Goumans, A. Wander, W. A. Brown and C. R. A. Catlow, *Phys. Chem. Chem. Phys.*, 2007, **9**, 2146-2152.
20. S. Nangia, N. M. Washton, K. T. Mueller, J. D. Kubicki and B. J. Garrison, *J. Phys. Chem. C*, 2007, **111**, 5169-5177.
21. T. S. Mahadevan and S. H. Garofalini, *J. Phys. Chem. C*, 2008, **112**, 1507-1515.
22. P. Ugliengo, M. Sodupe, F. Musso, I. J. Bush, R. Orlando and R. Dovesi, *Adv. Mater.*, 2008, **20**, 4579-4583.
23. F. Musso, M. Sodupe, M. Corno and P. Ugliengo, *J. Phys. Chem. C*, 2009, **113**, 17876-17884.
24. E. R. Cruz-Chu, A. Aksimentiev and K. Schulten, *J. Phys. Chem. B*, 2006, **110**, 21497-21508.
25. Z. Du and N. H. De Leeuw, *Dalton Trans.*, 2006, 2623-2634.
26. A. A. Hassanali and S. J. Singer, *J. Phys. Chem. B*, 2007, **111**, 11181-11193.
27. D. Argyris, D. R. Cole and A. Striolo, *J. Phys. Chem. C*, 2009, **113**, 19591-19600.
28. R. Notman and T. R. Walsh, *Langmuir*, 2009, **25**, 1638-1644.

29. S. Romero-Vargas Castrillon, N. Giovanbattista, I. A. Aksay and P. G. Debenedetti, *J. Phys. Chem. B*, 2009, **113**, 1438-1446.
30. J. C. Fogarty, H. M. Aktulga, A. Y. Grama, A. C. T. van Duin and A. S. Pandit, *J. Chem. Phys.*, 2010, **132**, 174704.
31. W. A. Adeagbo, N. L. Doltsinis, K. Klevakina and J. Renner, *ChemPhysChem*, 2008, **9**, 994-1002.
32. K. Leung, I. M. B. Nielsen and L. J. Criscenti, *J. Am. Chem. Soc.*, 2009, **131**, 18358.
33. A. Tilocca and A. N. Cormack, *ACS Appl. Mater. Inter.*, 2009, **1**, 1324-1333.
34. A. A. Skelton, P. Fernter, J. D. Kubicki, D. J. Wesolowski and P. T. Cummings, *J. Phys. Chem. C*, 2011, **115**, 2076-2088.
35. A. A. Skelton, D. J. Wesolowski and P. T. Cummings, *Langmuir*, 2011, **27**, 8700-8709.
36. G. Kresse and J. Furthmüller, *Phys. Rev. B*, 1996, **54**, 11169.
37. G. Kresse and J. Furthmüller, *Comput. Mater. Sci.*, 1996, **6**, 15.
38. P. E. Blochl, *Phys. Rev. B*, 1994, **50**, 17953.
39. G. Kresse and D. Joubert, *Phys. Rev. B*, 1999, **59**, 1758.
40. J. P. Perdew, K. Burke and M. Ernzerhof, *Phys. Rev. Lett.*, 1996, **77**, 3865.
41. J. C. Grossman, E. Schwegles, E. W. Draeger, F. Gygi and G. Galli, *J. Chem. Phys.*, 2004, **120**, 300-311.
42. P. H.-L. Sit and N. Marzari, *J. Chem. Phys.*, 2005, **122**, 204510.
43. S. B. Rempe, T. R. Mattsson and K. Leung, *Phys. Chem. Chem. Phys.*, 2008, **10**, 4685.
44. P. Ugliengo, D. Viterbo and G. Chiari, *Z. Kristallogr.*, 1993, **208**, 383-383.
45. M. G. Tucker, D. A. Keen and M. T. Dove, *Mineral. Mag.*, 2001, **65**, 489-507.
46. W. W. Schmahl, I. P. Swainson, M. T. Dove and A. Graeme-Barber, *Z. Kristallogr.*, 1992, **201**, 125-145.
47. G. Hura, J. M. Sorenson, R. M. Glaeser and T. Head-Gordon, *J. Chem. Phys.*, 2000, **113**, 9140.
48. J. M. Sorenson, G. Hura, R. M. Glaeser and T. Head-Gordon, *J. Chem. Phys.*, 2000, **113**, 9149.
49. T. Todorova, A. P. Seitsonen, J. Hutter, I.-F. W. Kuo and C. J. Mundy, *J. Phys. Chem. B*, 2006, **110**, 3685-3691.
50. P. Mignon, P. Ugliengo, M. Sodupe and E. R. Hernandez, *Phys. Chem. Chem. Phys.*, 2010, **12**, 688-697.
51. S. W. Ong, X. L. Zhao and K. B. Eisenthal, *Chem. Phys. Lett.*, 1992, **191**, 327.
52. Y. Duval, J. A. Mielczarski, O. S. Pokrovsky, E. Mielczarski and J. J. Ehrhardt, *J. Phys. Chem. B*, 2002, **106**, 2937-2945.
53. V. Ostroverkhov, G. A. Waychunas and Y. R. Shen, *Phys. Rev. Lett.*, 2005, **94**, 046102.
54. F. Musso, M. Sodupe and P. Ugliengo, *J. Phys. Chem. A*, 2011, **115**, 11221-11228.
55. O. Mo, M. Yanez and J. Elguero, *J. Chem. Phys.*, 1992, **97**, 6628-6638.
56. L. Gonzalez, O. Mo and M. Yanez, *J. Chem. Phys.*, 1998, **109**, 139-150.
57. L. Gonzalez, O. Mo and M. Yanez, *J. Chem. Phys.*, 1999, **111**, 3855-3861.
58. L. Gonzalez, O. Mo, M. Yanez and J. Elguero, *Theochem-J. Mol. Struct.*, 1996, **371**, 1-10.
59. H. Kleeberg, D. Klein and W. A. P. Luck, *J. Chem. Phys.*, 1987, **91**, 3200-3203.
60. P. Gilli, V. Bertolasi, V. Ferretti and G. Gilli, *J. Am. Chem. Soc.*, 1994, **116**, 909-915.

61. O. Mo, M. Yanez, J. E. Del Bene, L. Alkorta and J. Elguero, *ChemPhysChem*, 2005, **6**, 1411-1418.
62. L. Rincon, R. Almeida, D. Garcia-Aldea and H. D. Y. Riega, *J. Chem. Phys.*, 2001, **114**, 5552-5561.
63. S. S. Xantheas, *Chem. Phys.*, 2000, **258**, 225-231.
64. A. Schäfer, H. Horn and R. Ahlrichs, *J. Chem. Phys.*, 1992, **97**, 2571-2577.
65. R. Bukowski, K. Szalewicz, G. C. Groenenboom and A. van der Avoird, *J. Chem. Phys.*, 2008, **128**.
66. K. Szalewicz, C. Leforestier and A. van der Avoird, *Chem. Phys. Lett.*, 2009, **482**, 1-14.